Asian Journal of Chemistry; Vol. 35, No. 9 (2023), 2131-2142

ASIAN JOURNAL OF CHEMISTRY

https://doi.org/10.14233/ajchem.2023.28096

PANI/Short Nylon Fiber/Natural Rubber Conducting Composites: Dielectric Properties

SARITHA CHANDRAN A

Department of Chemistry and Centre for Research, St. Teresa's College (Autonomous), Ernakulam, Kerala-682011, India

Corresponding author: E-mail: sarithachandran@teresas.ac.in

Received: 3 June 2023; *Accepted*: 11 July 2023; *Published online*: 31 August 2023; AJC-21354

Polyaniline/polyaniline coated short nylon fibre/natural rubber (PANI/PANI-N/NR) and PANI/NR conductive polymer composites (CPCs) were prepared by mechanical mixing on a two-roll mill. PANI-N provides both conductivity and good mechanical properties to the CPCs. Such CPCs exhibiting improved mechanical properties are anticipated to have numerous applications in various devices. The frequency and temperature dependence of dielectric properties of polyaniline (PANI), natural rubber (NR), PANI/NR and PANI/PANI-N/NR CPCs in the frequency range 0.1 to 8 MHz and in the temperature range of 303 to 393 K, were investigated. Different theoretical equations and mixture equations were applied to fit the observed dielectric data of the prepared CPCs.

Keywords: Dielectric properties, Dielectric permittivity, Dielectric loss factor, AC conductivity, Conducting polymer composites,

INTRODUCTION

New high-dielectric constant materials that combine desirable dielectric qualities with adequate mechanical strength and processing ease are needed for the development of electronic devices operating at high operating frequencies, such as fast computers, cell phones and other such devices [1,2]. Making embedded capacitors for integrated electronic devices, in particular, calls for materials with high dielectric constants [3,4]. It is challenging to produce a material with the specific blend of mechanical and dielectric properties in a single component. Pure polymers are simple to work with mechanically durable components, although they often have low dielectric constants [5].

However, common high dielectric constant materials, including ferroelectric ceramics, are brittle and need high temperature processing, which is frequently incompatible with the state of circuit integration technology [6]. Designing a high dielectric constant material that is mechanically strong and processable at room temperature would be the optimal way to create such a one-component substance. This has increased interest in hybrid materials that combine the desirable features of the constituents, such as conducting polymer/polymer composites and polymer/ceramic composites.

The electronics industry has conducted substantial research on conducting polymer systems, which consist of a conducting polymer spread inside an insulating polymer matrix [7-10]. These materials can be employed in a wide variety of device applications due to their excellent mechanical properties, fascinating electrical properties and high dielectric constants.

A high dielectric constant can be attained using polyaniline (PANI) and various PANI/polymer blends, according to some studies. For instance, a partly crystalline PANI sample system [11] has a dielectric constant of $\geq 10^4$. For this system, an inhomogeneous disorder model was put forth, in which a region of ordered (crystalline) structure, defined by 3D metallic states, is coupled to a region of amorphous polymer chains, where 1D disorder-induced localization predominates. Camphor sulfonic acid (CSA), dodecylbenzene sulfonic acid (DBSA) and polystyrene sulfonic acid (PSSA) were used by Das *et al.* [12] to make three composites. In the frequency range of 42 kHz–2 MHz and the temperature range of 300-330 K, the dielectric and AC conductivity measurements of the undoped and doped PANI were investigated. For all PANI composites, the dielectric constant increased as the temperature rose. This indicated the increase in mobility of the electric dipoles in the polymers. When compared to interfacially polymerized nanofibres, the dielectric constant for DBSA doped PANI was over 5000, which is significantly greater than that of undoped PANI, where this value is roughly 800. The AC conductivity of the composites was found to be significantly higher.

Dash *et al*. [13] prepared novel multifunctional conductive blends and nanocomposites based on thermoplastic polyurethane (TPU), polyaniline (PANI) and functionalized single-wall carbon nanotubes (SWCNT) with excellent dielectric, mechanical and thermal properties. The TPU/PANI blend's improved thermal stability over PANI supports the development of chemical connections at the interface. A wide variety of applications have investigated the impact of PANI loading and temperature on the dielectric relaxation behaviour. In a broad frequency range (1–10^6 Hz), the impact of PANI loading and temperature on the dielectric relaxation behaviour has been investigated. The increased value of dielectric permittivity has verified how easy it is to polarize the dipoles in PANI and SWCNT. When compared to an unfilled TPU/PANI mixture, the dielectric permittivity and AC conductivity of TPU/PANI/SWCNT nanocomposites showed a significant improvement at an extremely low SWCNT loading level (0.5 wt%).

Rozik & El-Messieh [14] conducted dielectric and electrical conductivity tests on polystyrene and polyaniline (PS/PANI) blends made by casting. By increasing the PANI content in the PS/PANI blends, the values of increased, but they remained within the range of (10^{-10} S cm^{-1}), leading to the conclusion that PS/PANI with a concentration of 10% PANI held the best electrical properties. The second step involved selecting the best PS/PANI blend to combine with polyionic liquid in order to get improved performance. According to their research, the values of AC conductivity improved by two decants to be in the range of 10^{-8} S cm^{-1}, which is much beyond the threshold for usage in electrostatic dissipation applications.

The electrical properties of polyaniline/polyimide blends [15], polyaniline/polychloroprene composite [16], polyaniline/polyvinyl chloride blends [17] were also reported. The dielectric behaviour of conducting composites depends mainly on the method of preparation, conductivity, molecular structure, particle size and crystal structure [18-20]. It also depends on external factors such as frequency of the applied voltage, temperature, pressure and humidity [21,22]. Since the properties of the conducting polymers and conducting polymer composites (CPCs) are very much dependent on the microstructure, nature of dopant used, type of matrix and the processing variables, study of dielectric properties of these materials assume significance. Dielectric properties of polymers and polymer composites, like those of other dielectric materials are usually expressed in terms of its resistivity, condu-ctivity and complex permittivity. These quantities are functions of temperature and the type *i.e.* AC/DC and magnitude of the voltage applied [23-25]. Frequency and temperature dependence of dielectric properties of the CPCs throw light on the dielectric polarization and on the conduction mechanisms.

In this work, the polyaniline/natural rubber conducting polymer composites (PANI/NR CPCs) and PANI/polyaniline coated short nylon fiber/natural rubber composites (PANI/PANI-N/NR CPCs) were prepared by mechanical mixing. The details of the preparation and their characterization are described elsewhere [26]. It was found that the PANI/PANI-N/NR CPCs had improved mechanical characteristics and high conductivity. If these CPCs also possess good dielectric properties, they can be employed in a variety of device applications. In this study, the dielectric characteristics of PANI, NR and PANI/PANI-N/NR CPCs were examined in relation to frequency and temperature. Different theoretical equations and mixture equations are applied to fit the observed dielectric data of the CPCs.

EXPERIMENTAL

Sample preparation: Preparation of PANI and PANI coated short nylon fibres (PANI-N) has been reported earlier [26]. The PANI/NR and PANI/PANI-N/NR composites were prepared using a two-roll mill through mechanical mixing. Table-1 contains the preparation formula for the composites. Two series of CPCs were prepared, first with varying amounts of PANI (P-series) and the second with varying amounts of PANI-N (F-series), their cure parameters, cure kinetics, filler dispersion, mechanical, electrical and thermal characteristics are reported earlier [27].

TABLE-1
FORMULATION FOR THE PREPARATION OF CPCs

Ingredients (phr*)	P series				F series		
	NP_0	NP_1	NP_2	NP_3	NF_1	NF_2	NF_3
NR	100	100	100	100	100	100	100
PANI	0	40	90	140	90	90	90
PANI-N#	0	0	0	0	40	80	120

*Parts per hundred rubber, #PANI coated etched fiber, All the mixes contain Stearic acid- 1 phr and DCP- 3 phr.

Dielectric measurements

Method of measurements: The dielectric constant or permittivity is defined as the ratio of the field strength in vacuum to that in the material for the same distribution of charges. Dielectric constant is dependent on parameters like temperature, orientation, molecular structure of the material and frequency of the applied field. An electrical conductor charged with a quantity of electricity q at a potential V is said to have a capacity C = q/V. The capacity of a sample parallel plate capacitor is given by:

$$C = \frac{\varepsilon A}{d} \quad (1)$$

where A is the area of the parallel plates, d is the separation between the plates and ε is the ratio of dielectric constant of the medium between the plates to that of free space. When a parallel plate capacitor with a dielectric in between is charged, then the capacitance (C) is given by:

$$C = \frac{\varepsilon_o \varepsilon_r A}{d} \quad (2)$$

where A is the area of sample, d is the separation between the plates, ε_o is the permittivity of free space and ε_r is the dielectric constant of the material between the plates. Dielectric constant of the samples can thus be calculated if the capacitance, area and thickness of the samples are known. Thus, dielectric constant is presented as:

$$\varepsilon_r = \frac{Cd}{\varepsilon_o A} \quad (3)$$

The AC electrical conductivity can be calculated utilizing the dielectric parameters using eqn. 4:

$$\sigma_{AC} = 2\pi f \tan \delta \delta \varepsilon_o \varepsilon_r \quad (4)$$

where f is the frequency of the applied field and tan δ is the loss factor. The principle and theory underlying the evaluation of σ_{AC} from dielectric measurements is based on a treatment dealt by Goswamy [28].

Cell measurements: The dielectric properties of the CPCs were studied using a dielectric cell and an impedance analyzer, Hewlett Packard 4192A. The cell was standardized using Teflon pellets and lead. The fringe capacitance was eliminated by employing a procedure suggested by Ramasasthry *et al.* [29]. The samples, in the form of pellets of diameter 12 mm and ~ 2 mm thickness were mounted in between two copper disc electrodes. The capacitance of the samples was measured in the frequency range 0.1 to 8 MHz and in the temperature range 303 to 393 K. The data acquisition was automated by interfacing the impedance analyzer with a computer. For this, a virtual instrumentation package, based on a graphical programme was employed. This package is called LabVIEW, a base software package for implementing the virtual instrumentation and G programming. After obtaining capacitance and dielectric loss from the instrument, the LabVIEW software first calculates the dielectric constant and then evaluates the AC conductivity of the samples.

RESULTS AND DISCUSSION

Dielectric permittivity

Frequency dependence of pristine PANI: Fig. 1 presents the variation of dielectric permittivity (ε′) *i.e.* the real part of complex permittivity, of pristine PANI with frequency. The permittivity decreases with increase in frequency at all temperatures. This is more pronounced at low frequencies. Finally, it reaches a constant value at all temperatures. The decrement in permittivity with increase of frequency reveals that the systems exhibit strong interfacial polarization at low frequencies. As reported by other authors, the strong low frequency dispersion of permittivity is a characteristic of charged carrier systems [30]. This is the normal behaviour found in the case of PANI [31] and such behaviour can be explained on the basis of Maxwell-Wagner theory for interfacial polarization [32].

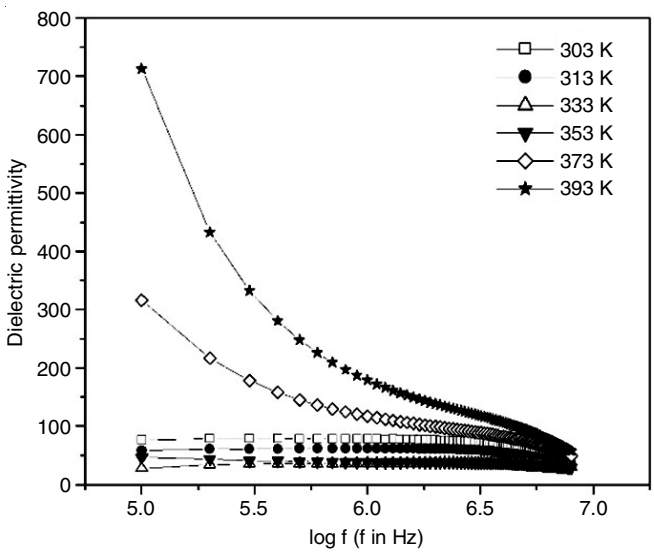

Fig. 1. Variation of dielectric permittivity of PANI with frequency

Temperature dependence of pristine PANI: Fig. 2 shows the variation of dielectric permittivity of pristine PANI with temperature at different frequencies. Generally, at any particular frequency, the dielectric permittivity decreases with temperature up to 333 K and then increases with increasing temperature. This behaviour is more pronounced at lower frequencies.

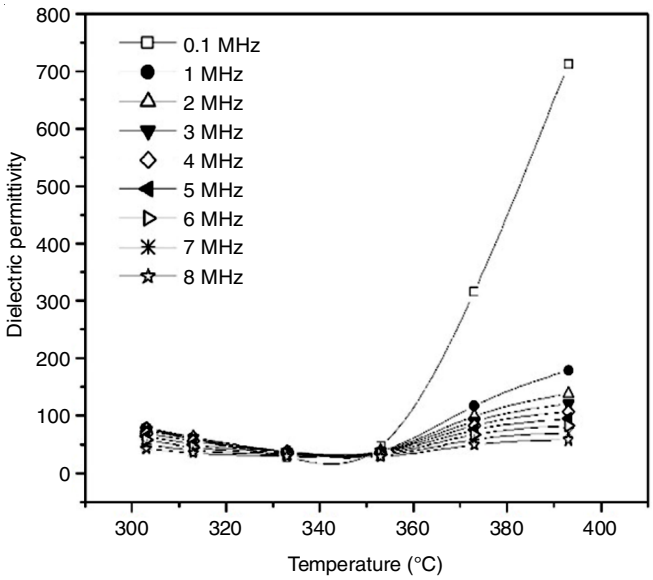

Fig. 2. Variation of dielectric permittivity of PANI with temperature

Dielectric behaviour of conducting polymers depends on their structure. PANI aggregates are made up of small grains, which are formed from still smaller primary particles. These primary particles have a metallic core surrounded by an amorphous non-metallic shell. This forms a heterogeneous structure as put forward by Maxwell-Wagner. In the Maxwell-Wagner model, well conducting grains are separated by poorly conducting grain boundaries. The increasing permittivity value with increasing temperature is in accordance with Maxwell-Wagner theory, which means that at higher temperatures, Maxwell-Wagner type of polarization is predominant. It can be seen from Fig. 3 that at 303 K, PANI has a permittivity of 76 and at 393 K, the value is 712 at 0.1 MHz. The high values of dielectric permittivity at lower frequencies can be accounted for by employing Koop's theory, which is based on Maxwell-Wagner model for heterogeneous double layer dielectric structures [33-35].

Frequency dependence of dielectric loss factor of pristine PANI: The variation of dielectric loss factor (ε″), *i.e.* the imaginary part of complex permittivity with frequency is presented in Fig. 3. It decreases with frequency at all temperatures as in the case of dielectric permittivity and reaches a constant value. The decrease is more pronounced at lower frequencies, since the dependence of loss factor of PANI with frequency appears as straight lines at lower frequencies, at low temperatures. Beyond 353 K, deviation from straight line is observed.

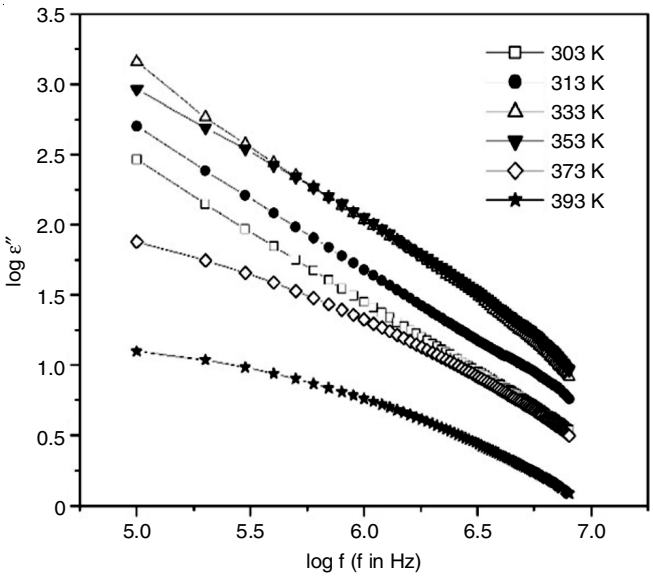

Fig. 3. Variation of dielectric loss factor with frequency

The loss factor (ε''_{obs}) must be regarded as the sum of contributions of three distinct effects [36] as:

$$\varepsilon''_{obs} = \varepsilon''_{DC} + \varepsilon''_{MW} + \varepsilon''_{D} \quad (5)$$

where ε''_{DC} is due to DC conductance, ε''_{MW} is due to interfacial polarization and ε''_{D} is the usual dipole orientation or Debye loss factor. Different mathematical equations have been developed to distinguish between loss arising from a DC conductivity process and from other sources of different processes. These equations were developed by considering the sample as parallel resistor-capacitor circuit [37-39]. The loss factor due to DC conductance (ε''_{DC}) is given by eqn. 6 [38]:

$$\varepsilon''_{DC} = \frac{1.8\times10^{12}[G_{spec}]}{f} \quad (6)$$

where G_{spec} is the specific conductivity (S/cm) of the sample. The loss factor due to the Maxwell-Wagner or interfacial polarization (ε''_{MW}) is represent by eqn. 7 [40]:

$$\varepsilon''_{MW} = \varepsilon_{\infty}\left(1+\frac{K}{1+\omega^2\tau^2}\right) \quad (7)$$

where ε_{∞} and K were calculated by considering two different dielectric permittivity of the sample at the interfaces and τ is the relaxation time of the interfacial polarization. By expressing the above two equations in logarithm form and making the plot of log ε''_{DC} and log ε''_{MW} *vs.* logarithm of frequency, two different curves will be obtained. The log ε''_{DC} *vs.* log f represents a straight line and the log ε''_{MW} *vs.* log f represents a sigmoidal curve.

Fig. 3 shows that at lower frequencies and temperatures, the loss factor (ε''_{obs}(decrease linearly with increasing frequency. These results suggest that DC conductivity process is more significant than interfacial polarization at these frequencies and temperatures [31].

Generally, it is believed in dielectric analysis that the high frequency permittivity (dielectric constant) is mainly associated with dipolar relaxation, whereas at lower frequency and higher temperature, the contributions of interfacial polarization (Maxwell-Wagner type of polarization) and DC conductivity become more significant in both ε′ and ε″. Interfacial polarization arises mainly from the existence of polar and conductive regions dispersed in relatively less polar and insulating matrix. This phenomenon is particularly important in conjugated polymers and may interfere on the relaxation process analysis. Therefore, several authors prefer to describe the dielectric properties of these systems by using the electric modulus formalism [30,41-44]. The complex electric modulus is derived from the complex permittivity, according to the relationship defined by Macedo *et al.* [45]. The real and imaginary parts of the electric modulus (M′ and M″) can be calculated from ε′ and ε″, as follows [46]:

$$M' = \frac{\varepsilon'}{(\varepsilon')^2 + (\varepsilon'')^2} \quad (8)$$

$$M'' = \frac{\varepsilon''}{(\varepsilon')^2 + (\varepsilon'')^2} \quad (9)$$

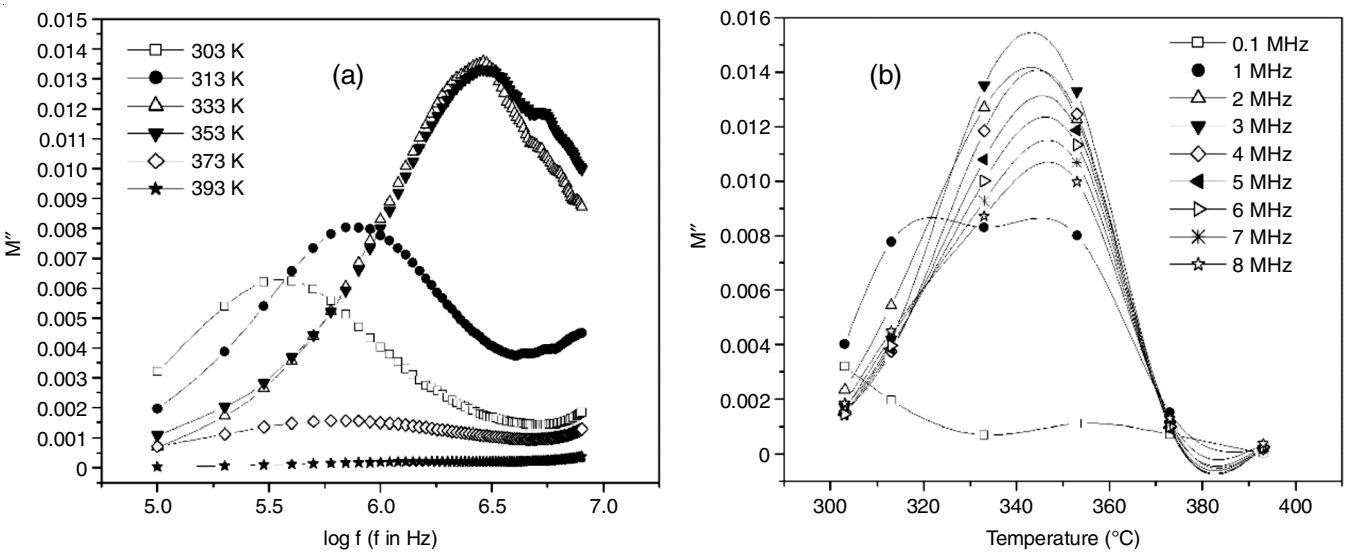

Fig. 4. Imaginary part of electric modulus of pristine PANI (a) isothermal plots (b) isochronal plots

The electric modulus representations of dielectric process give us some idea of relaxation of dipoles that exists in different energy environments, independent of the strong effect of DC conductivity, which often mask the actual dielectric relaxation processes active in these types of systems. Fig. 4 shows the isothermal and isochronal dependence of the imaginary part of electric modulus (M″) with frequency and temperature, respectively, of pristine PANI. PANI exhibits only one broad peak, both in isothermal and isochronal plots with a narrow distribution of the relaxation, indicating a uniform system and a single relaxation process. The peak shifts to higher frequencies in the isothermal plots with increasing temperature upto 333 K. With increasing frequency, the peak height increases initially upto 3 MHz, which then decreases.

Effect of frequency and temperature of natural rubber (NR) gum vulcanizate: The frequency and temperature dependence of NR gum vulcanizates is shown in Fig. 5. As frequency increases, dielectric permittivity decreases at all temperatures. The decrease is gradual at lower frequencies and more significant at higher frequencies. The dielectric constant of the unvulcanized NR is reported to be in the range 2.6 to 3.04 [47]. A dielectric constant of 2.3 is obtained at 0.1 MHz in the present study.

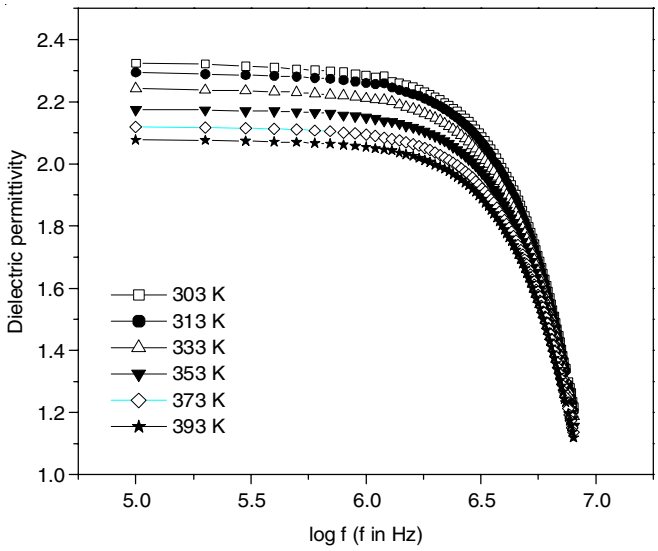

Fig. 5. Variation of dielectric permittivity of NR gum vulcanizate with (a) frequency (b) temperature

The dielectric behaviour of a polymeric material under the influence of an external electric field depends on the polarization effect that occurs within the material. The total polarization is the sum of the deformational polarization and orientational polarization. At low applied frequencies, both factors contribute to the total polarization. As the frequency increased, the orientation polarization becomes out of phase with the applied field *i.e.* the dipolar motion can no longer follow the rapid vibration in the electric field. So, the dielectric permittivity of polymeric materials decreases with increase in applied frequency. The polarization and hence the dielectric permittivity must be regarded as complex quantity:

$$\varepsilon^* = \varepsilon' - i\varepsilon'' \quad (10)$$

The complex dielectric permittivity (ε^*) is given by the Debye equation as follows:

$$\varepsilon^* = \varepsilon_\infty + \frac{\varepsilon_o - \varepsilon_\infty}{1 + i\omega\tau} \quad (11)$$

where ω is the angular frequency, ε_o is the static dielectric permittivity and ε_∞ is the dielectric permittivity at infinite frequency. The real and imaginary components ε′ and ε″ are given by [48-50]:

$$\varepsilon' = \varepsilon_\infty + \frac{\varepsilon_o - \varepsilon_\infty}{1 + (\omega\tau)^2} \quad (12)$$

$$\varepsilon'' = \frac{(\varepsilon_o - \varepsilon_\infty)\omega\tau}{1 + (\omega\tau)^2} \quad (13)$$

According to eqn. 12, the dielectric permittivity decreases with increase in frequency and the decrease is more pronounced at higher frequencies.

The temperature dependence of NR gum vulcanizates is shown in Fig. 6. The dielectric permittivity is found to decrease with increase in temperature at all frequencies. When the temperature increases, due to thermal expansion of matter, the ratio of the number of molecules to the effective length of the dielectric diminishes and as a result, dielectric permittivity decreases [36,51]. In other words, as the temperature increases, the polymer density reduces which, in turn causes a decrease in dielectric permittivity.

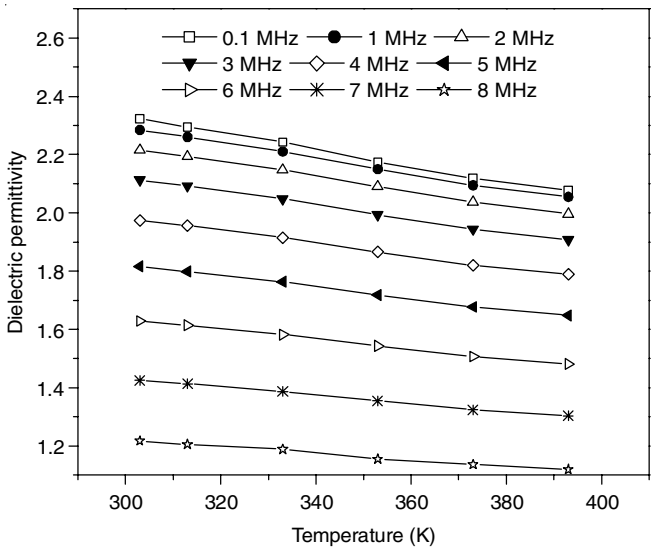

Fig. 6. Variation of dielectric permittivity of NR gum vulcanizate with temperature

Frequency dependence of the CPCs: The dielectric properties of NR/PANI (P series) and NR/PANI/PANI-N (F-series) composites containing different loadings of PANI and PANI-N, respectively, were studied at different temperatures in the frequency range 0.1-8 MHz. The effect of frequency on the dielectric permittivity of NR composites NP_2, NP_3 and the F-series composite NF_3 at some selected temperatures is represented in Fig. 7. This indicates that more and more PANI dipoles can no longer keep up with the increasing frequency. This

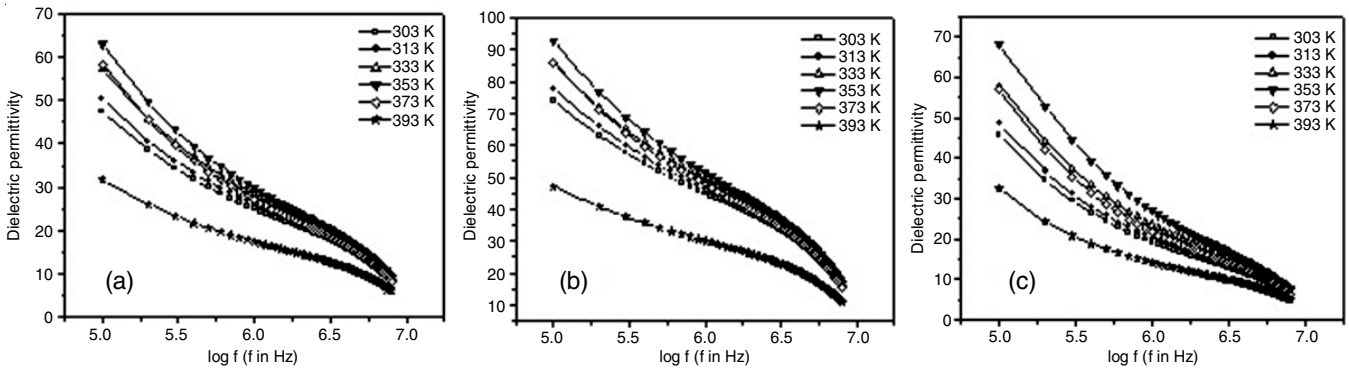

Fig. 7. Effect of frequency on the dielectric permittivity of CR/PANI composite (a) NP_2, (b) NP_3, (c) NF_3

behaviour is in accordance with Maxwell-Wagner interfacial polarization. As the frequency of the applied field increases, interfacial polarization decreases and hence dielectric permittivity decreases. The absolute value of the dielectric permittivity of the CPCs is found to be much greater than the gum vulcanizate. Higher values are obtained for composites with higher PANI loading. Dielectric constants as high as 47, 73 and 45 are obtained for NP_2, NP_3 and NF_3 composites, respectively at 0.1 MHz. Compared to most of the polymers which have ε′ values between 2 and 10 (ε′ = 10 for PVDF; ε′ = 5.6 for PU) and many common ceramics such as SiO_2 (ε′ = 4.0) and Si_3N_4 (ε′ = 7.0), the results obtained by NR based CPCs are quite remarkable.

Temperature dependence of the CPCs: The effect of temperature on the dielectric permittivity of the composites NP_2, NP_3 and NF_3 at some selected frequencies is presented in Fig. 8. In all the three composites, the dielectric permittivity is found to increase initially with temperature up to 353 K and then decreases. This effect is more pronounced at lower frequencies and nominal at higher frequencies.

The high dielectric permittivity at low frequencies found at high temperatures may be explained by the presence of permanent dipole moments indicating a small effective charge separation. Such a small separation must be due to asymmetry in the fields experienced by the presence of charged ions. In most cases, the atoms or molecules in the samples cannot orient themselves at low temperature region. When the temperature rises, the orientation of these dipoles is facilitated and this increases the dielectric polarization. At even high temperatures, the chaotic thermal oscillations of molecules are intensified and the degree of orderliness of their orientation is diminished and thus the permittivity passes through a maximum value. In present case, this maximum temperature is 353 K. At very high temperatures, the dielectric permittivity decreases. This is due to the thermal expansion of the matrix as discussed earlier. At high frequencies, the temperature has little effect on dielectric permittivity [36,51].

Loading dependence of the CPCs: Variation of dielectric permittivity with PANI loading of P-series CPCs and PANI-N loading of F-series CPCs at 303 K are shown in Fig. 9. It is found to increase with increase in PANI and PANI-N content at all frequencies. The increase is more pronounced at lower frequencies. At 0.1 MHz, a maximum value of 73 is obtained at 140 phr PANI loading (CPC NP_3) and a value of 45 at 120 phr PANI-N loading (CPC NF_3). Thus, it is clear that the dielectric properties of the NR matrix get modified by addition of PANI and PANI-N and the required dielectric constant can be achieved by varying their concentration.

Tailoring of dielectric permittivity of the CPCs: Efforts were made to correlate the dielectric constant of the composite samples with those of pristine PANI and gum NR. Several mixture equations exist, which can be employed to predetermine the dielectric permittivity of the composites correctly [52]. For this, the dielectric has to be considered as a mixture of several components. The observed permittivity of the CPCs can be predicted in terms of the permittivity of the host matrix and that of the conducting polymer by using well-known empirical equations with certain modifications. Among the different

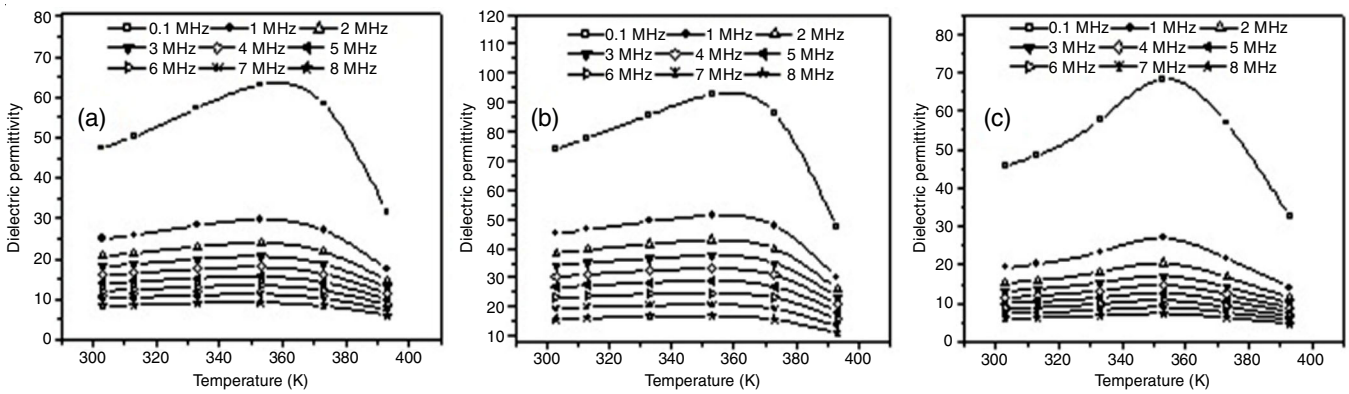

Fig. 8. Temperature dependence of dielectric permittivity of (a) NP_2, (b) NP_3, (c) NF_3

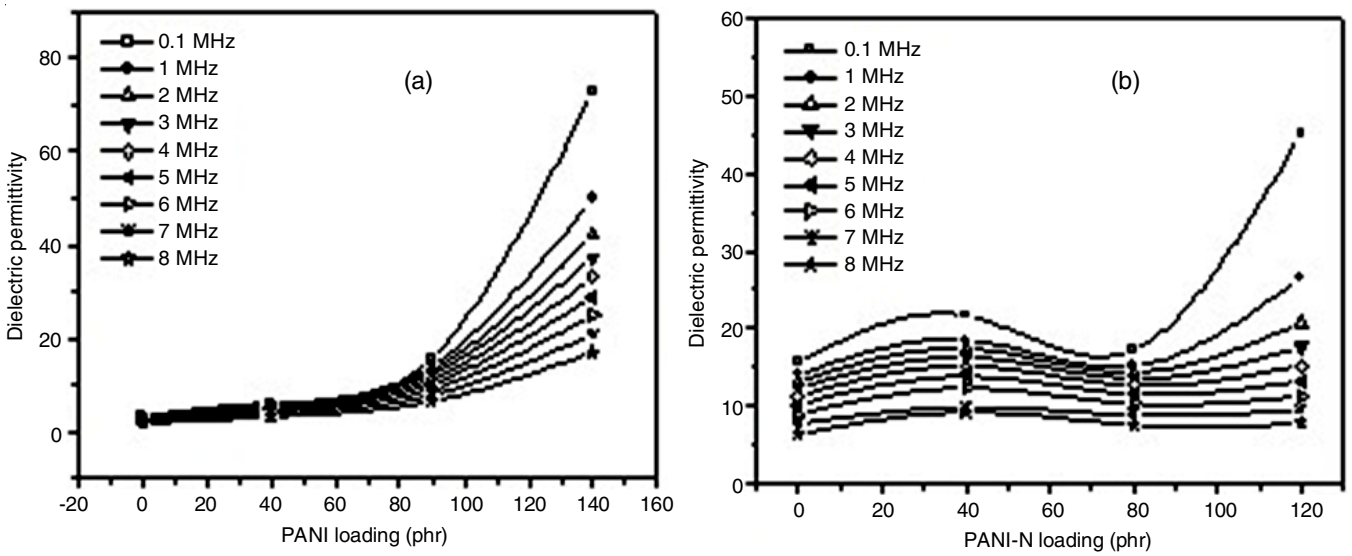

Fig. 9. Dielectric permittivity *vs.* (a) PANI loading of P-series CPC, (b) PANI-N loading of F-series CPC

mixture equations, the simplest one is the Lichtenecker equation [36,53-55], which can be represented as:

$$\log \varepsilon_{eff} = (1 - V_f) \log \varepsilon_m + V_f \log \varepsilon_f \quad (14)$$

where ε_{eff} is the dielectric permittivity of the composite, V_f is the volume fraction of the filler, ε_m and ε_f are the dielectric permittivity of the matrix and the filler respectively. The best-known formula for ε_{eff} for a binary mixture is associated with Maxwell and Wagner. Maxwell developed the idea of effective conductivity of a binary system consisting of spheres of a particular conductivity distributed uniformly in a continuum of different conductivity. Wagner adopted Maxwell's expression to the dielectric case and the equation is as follows [56]:

$$\varepsilon_{eff} = \varepsilon_m \frac{\left(1 - 2V_f \frac{(\varepsilon_m - \varepsilon_f)}{(2\varepsilon_m + \varepsilon_f)}\right)}{\left(1 + V_f \frac{(\varepsilon_m - \varepsilon_f)}{2\varepsilon_m + \varepsilon_f}\right)} \quad (15)$$

Another mixture equation of the form [57]:

$$\varepsilon_f = \frac{\varepsilon_m \varepsilon_f}{\varepsilon_m y_2 + \varepsilon_f y_1} \quad (16)$$

is also found to be useful in predicting the loading dependence of dielectric permittivity of the CPCs. Here, y_1 and y_2 represent the weight fractions of the matrix and the filler, respectively. For CPCs, the eqns. 14-16 did not fit well with the experimental data. Deviations may have occurred due to the formation of agglomerates of PANI particles in the matrix. Hence modified versions of the equations were derived assuming that spherical shaped conducting particles are well distributed in the non-conducting medium. These modified equations are employed to fit the experimental data. For convenience, the logarithmic values were calculated and plotted. The modified form of eqn. 14 used to calculate the dielectric permittivity of the CPCs is:

$$\log \varepsilon_{eff} = (1 - W_f)(\log \varepsilon_m)^k + W_f (\log \varepsilon_f)^k \quad (14a)$$

Eqns. 15 and 16 were also modified with an exponential factor as:

$$\log \varepsilon_{eff} = \log \varepsilon_m \frac{\left(1 - 2W_f \frac{(\varepsilon_m - \varepsilon_f)}{(2\varepsilon_m + \varepsilon_f)}\right)}{\left(1 + W_f \frac{(\varepsilon_m - \varepsilon_f)}{2\varepsilon_m + \varepsilon_f}\right)} + \log k \quad (15a)$$

$$\log \varepsilon_{eff} = \log \frac{\varepsilon_m \varepsilon_f}{\varepsilon_m y_2 + \varepsilon_f y_1} + \log k \quad (16a)$$

W_f is the weight fraction of the filler. Using eqns. 14a, 15a and 16a, log ε_{eff} was calculated and plotted against log f.

Fig. 10 shows the plots along with the plots of the experimentally observed values. It is clear that the estimated permittivity differs from the measured one at lower frequencies as the loading increases. For NR composites, the values of k in eqns. 14a, 15a and 16a are respectively between 0.6 and 1.3, 0.38 and 0.73 and 0.2 and 0.7. The values for CR composites range from 0.23 to 0.88. The difference in filler distribution and filler matrix interactions may account for the marginal variation of the empirical constant and the departure from the observed value at larger loadings.

AC conductivity: Given the vast range of electrical conductivity that dielectric materials exhibit, there are numerous mechanisms of carrier transport that can be used to explain the conductivity over the entire range. Various mechanisms have been put forth, each reflecting a different regime's evolution of the underlying electrical structure. The DC conductivity value at ambient temperature is insufficient to distinguish between these several models. The different conduction mechanisms can be distinguished by measurements of the frequency and temperature dependence of the AC conductivity (AC). Eqn. 4 was used to calculate the samples' AC conductivity values from the dielectric data.

The current has two components, the in-phase component I cos Φ and the out-of-phase component I sin Φ and may be

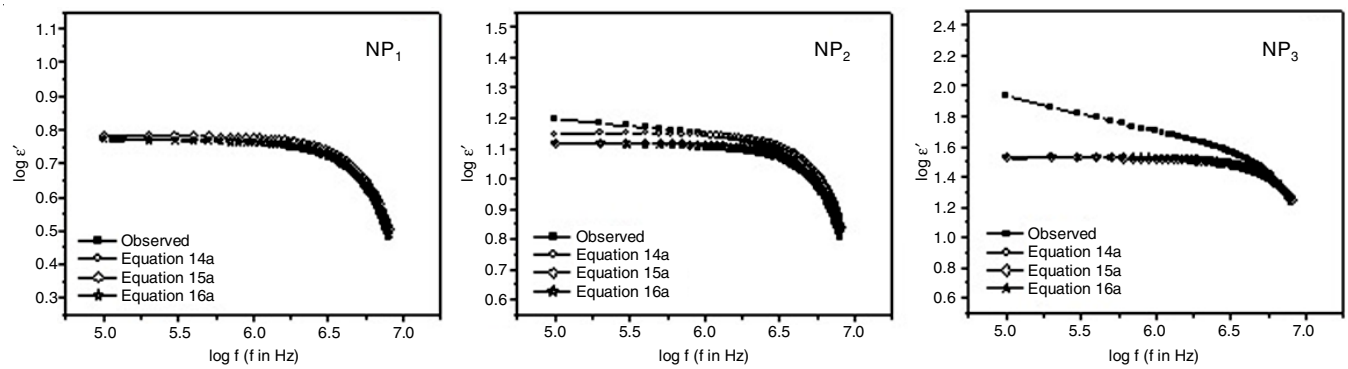

Fig. 10. log ε′ *vs.* log f at 303 K for the observed and calculated permittivity of NP_1, NP_2 and NP_3

calculated using Ohm's equation for a sample with thickness h and cross-sectional area A. The formulas by $\sigma'_{AC} = (h/A) I \cos \Phi$ and $\sigma''_{AC} = (h/A) I \sin \Phi$ are used to calculate the real and imaginary AC electrical conductivities, respectively. The two terms that make up the real part of AC conductivity are as follows:

$$\sigma'_{ac} = \sigma_1(T) + \sigma_2(\omega) \quad (17)$$

$$\sigma_1(T) = \sigma_o \exp\left(-\frac{E}{kT}\right) \quad (18)$$

$$\sigma_2(\omega) = B\omega^n \quad (19)$$

The first term, $\sigma_1(T)$ is related to drift electric charge carriers. It is frequency independent and temperature dependent and is really the DC electrical conductivity. The second term; $\sigma_2(\omega)$, is related to the dielectric relaxation caused by bound charge carriers. k is the Boltzmann's constant and E is the activation energy in eV. σ_o, B and n are constants, where n is temperature dependent and ω is the angular frequency of the applied field [46].

Frequency dependence of pristine PANI: Fig. 11 shows the variation in AC conductivity of pure PANI with frequency at various temperatures. It initially exhibits a nominal increase up to 2 MHz before decreasing at higher frequencies. The heterogeneous model or the Maxwell-Wagner two layers can be used to explain this. The heterogeneities of the material as described by the Maxwell-Wagner model consist of two layered capacitors *i.e.* well conducting grains separated by layers of lower conductivity. While the high frequency AC conductivity is a result of the conductive grains, the low-frequency AC conductivity is connected to the resistive grain borders. Electrical conductivity in conducting polymers is due to the hopping of charge carriers. The hopping of the charge carriers likewise increases as the frequency of the applied field does, enhancing conductivity. Eqns. 4 and 18 also explain how σ_{AC} rises as frequency rises. At high frequencies, greater than 2 MHz, AC conductivity decreases with increase in frequency as the hopping of charge carriers lags behind the applied frequency.

The variation of the exponent 'n' with temperature gives information on the specific mechanism involved in the conduction process. This behaviour has been ascribed to the inhomogeneity within the solid caused by the absence of long range crystalline order [58]. Fig. 12 presents a plot of log σ_{AC} against log f from 2 MHz to 8 MHz at various temperatures. On the basis of eqn. 19, which states that $\sigma(\omega) = B\omega^n$, where n is an index less than or equal to unity, it is possible to comprehend the kind of conduction/relaxation process that predominates in amorphous materials. The relationship between the exponent 'n' and temperature reveals the precise mechanism that is engaged in the conduction process. This behaviour has been ascribed

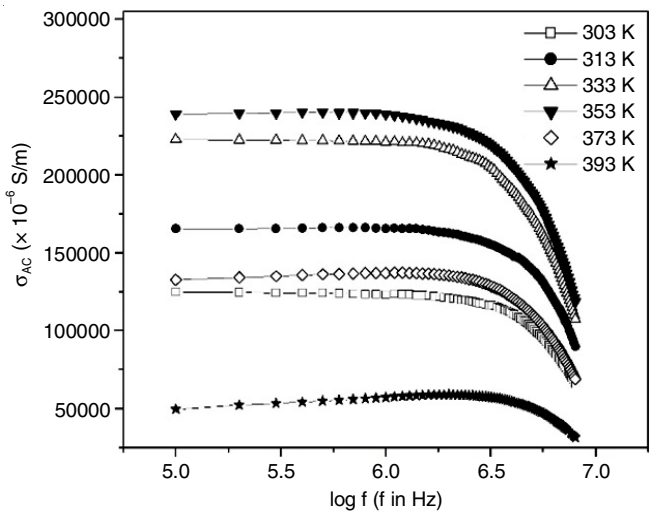

Fig. 11. Variation of AC conductivity of PANI with frequency

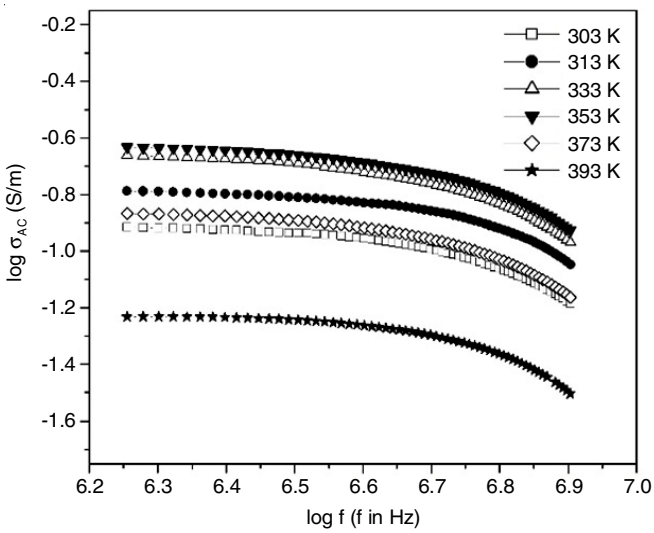

Fig. 12. log AC conductivity *vs.* log frequency of pristine PANI

to the inhomogeneity within the solid caused by the absence of long range crystalline order [54].

Carrier transport *via* hopping can be identified with this type of dielectric response. Jonscher [59] proposed that such a dependence on frequency and temperature represents a universal law, applicable to a very wide range of materials irrespective of their chemical and physical structure and the type of dominant charge carriers. The value of n obtained from the plots lies between -0.36 and -0.46 (Table-2). This value is in accordance with the theory of hopping conduction in amorphous materials. The observed frequency dependence suggests that the mechanism responsible for AC conduction in pristine PANI is hopping [60].

TABLE-2
n VALUES OF PRISTINE POLYANILINE

Temp. (K)	n values	Temp. (K)	n values
300	-0.40	353	-0.43
313	-0.36	373	-0.44
333	-0.46	393	-0.38

Temperature dependence of pristine PANI: Fig. 13 shows how temperature affects the AC electrical conductivity of pure PANI. The conductivity rises with rising temperature, reaches a maximum and then falls. The rise in the drift mobility of thermally activated electrons, which raises the hopping conduction, can be correlated with the increase in conductivity with temperature [61]. Mott's variable range hopping mechanism

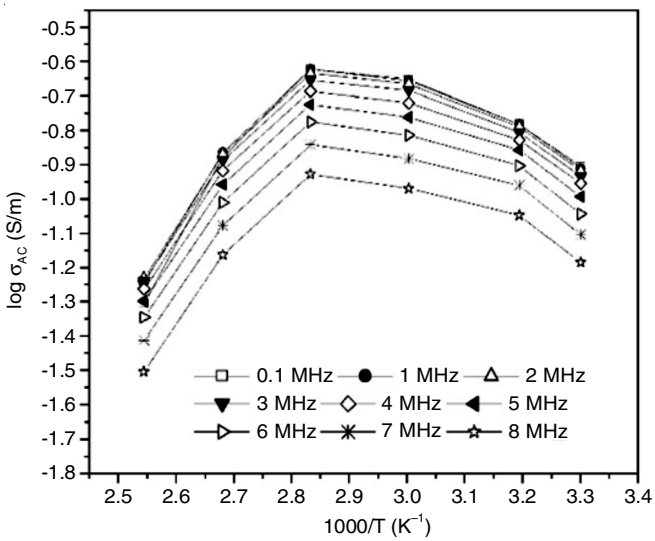

Fig. 13. log AC conductivity as a function of 1000/T for pristine PANI

(VRH) has been applied with varying degree of success to conducting organic systems [62-64].

The use of Mott's VRH model in polyaniline film has been demonstrated by Reghu *et al.* [65]. A conduction mechanism based on electron tunnelling between conducting grains embedded in an insulating matrix has also been used to explain the thermal variation in conductivity with time and temperature in PANI [66-68]. The thermal degradation was attributed to a decrease of the grain size with a simultaneous broadening of the barriers.

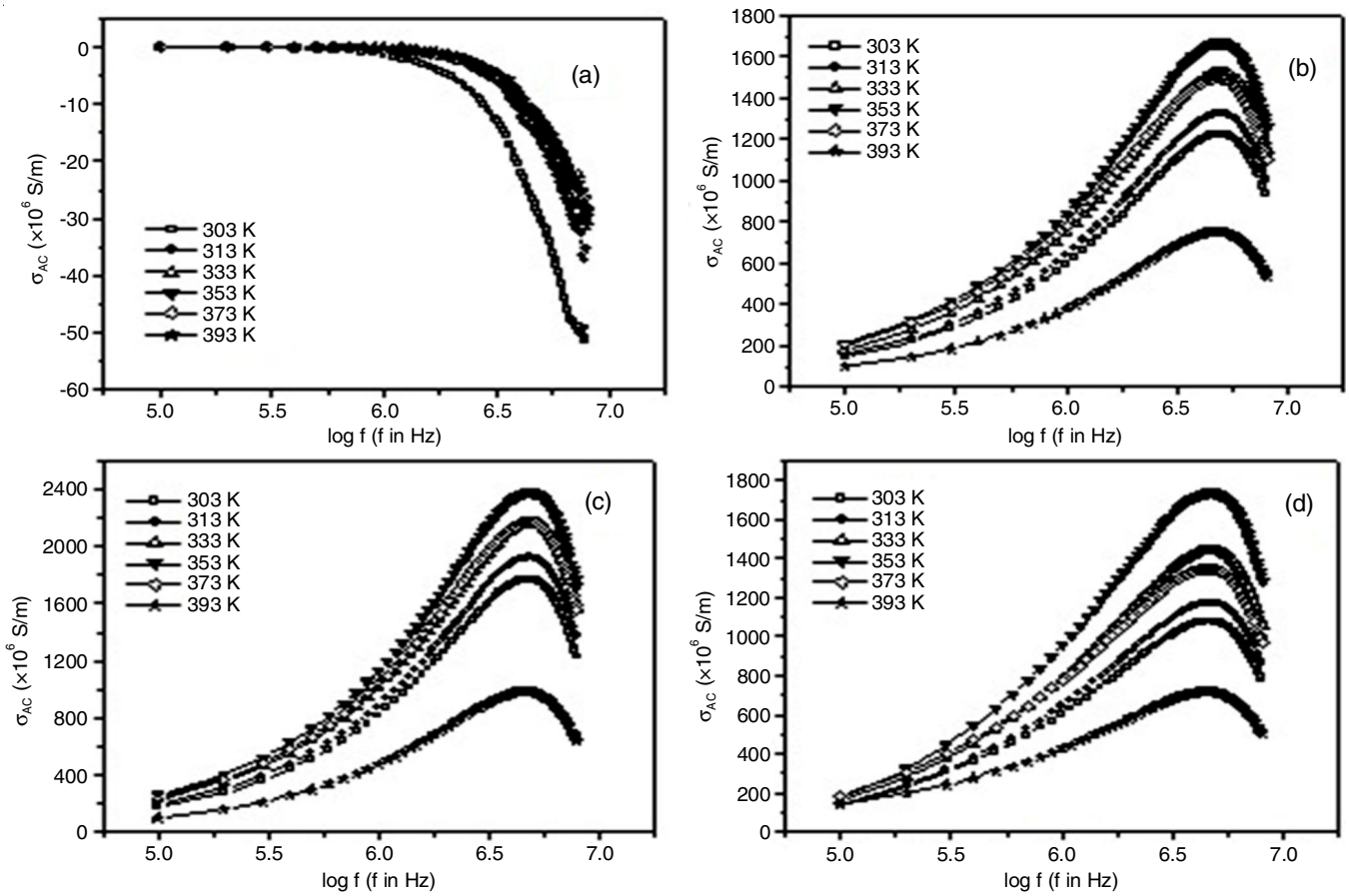

Fig. 14. Effect of frequency on the AC conductivity of (a) NR gum vulcanizate, (b) NP_2, (c) NP_3, (d) NF_3

Frequency dependence of NR based CPCs: Fig. 14 presents the effect of frequency on the AC conductivity of gum NR, P-series and F-series composites in the temperature range 303-393 K. Most of the polymeric materials are insulators and practically no conductivity is observed in unvulcanized elastomers.

At various temperatures, the CPCs with various PANI and PANI-N loadings exhibit comparable frequency dependency. As PANI and PANI-N are incorporated, the AC conductivity rises with frequency and then falls after reaching a maximum at higher frequencies. The rise in hopping conduction is what causes the conductivity of AC to increase with frequency. With increase in PANI loading, the AC conductivity shows an increase.

Effect of temperature of NR based CPCs: The effect of temperature on AC conductivity of the CPCs is plotted and presented in Fig. 15. Up to 353 K, the AC conductivity rises with temperature and then decreases. Although at very high temperatures the higher segmental mobility of the polymer may insulate the PANI particles and lower the conductivity, the initial rise in conductivity is attributable to the increase in hopping conduction.

Loading dependence of natural rubber based CPCs: Fig. 16 illustrates the impact of PANI and PANI-N loading on the AC conductivity of CPCs at 303 K at various frequencies. It rises as PANI and PANI-N loadings rise, as expected. The highest conductivity is noted for CPC with 140 phr PANI loading (NP_3) (2.13 10^{-3} S/m at 5 MHz). The conductivity of the 120 phr PANI-N-loaded composite (NF_3) is remarkably similar (1.68 10^{-3} S/m) to that of the NP_3 composite.

Conclusion

The dielectric properties of polyaniline (PANI) and the conductive polymer composites (CPCs) were measured in the frequency range 0.1 to 8 MHz and in the temperature range 303 to 393 K. PANI exhibits interfacial polarization at low frequencies, as shown by the fact that the dielectric permittivity of pure PANI falls as frequency rises. PANI exhibits a permittivity of 76 at 303 K at 0.1 MHz and reaches a maximum of 712 at 393 K. The loss factor of pure PANI drops linearly with frequency at low frequencies and temperatures, indicating that DC conductivity mechanism is more important than interfacial polarization at these frequencies and temperatures. Due to a reduction in interfacial polarization, the dielectric permittivity drops of CPCs with frequency and rises with PANI and PANI-N loading. It rises with rising temperature, reaches a maximum and then falls. A 150 phr PANI-loaded NR CPC exhibits a dielectric permittivity of up to 177 at 303 K and 0.1 MHz. The dielectric dispersion could be fitted well with the well-known empirical equations. One of these equations can be used to determine the effective permittivity of the prepared CPCs. The

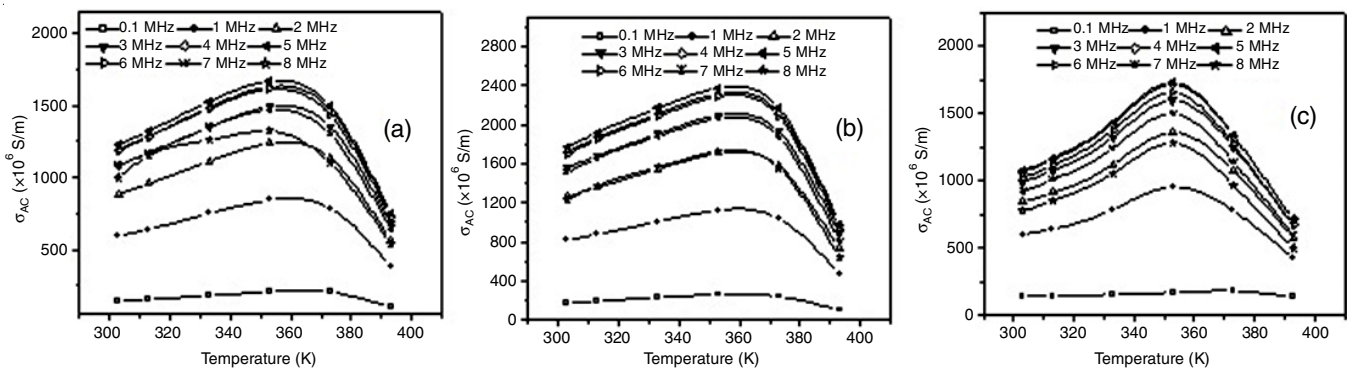

Fig. 15. Effect of temperature on the AC conductivity of (a) NP_2, (b) NP_3, (c) NF_3

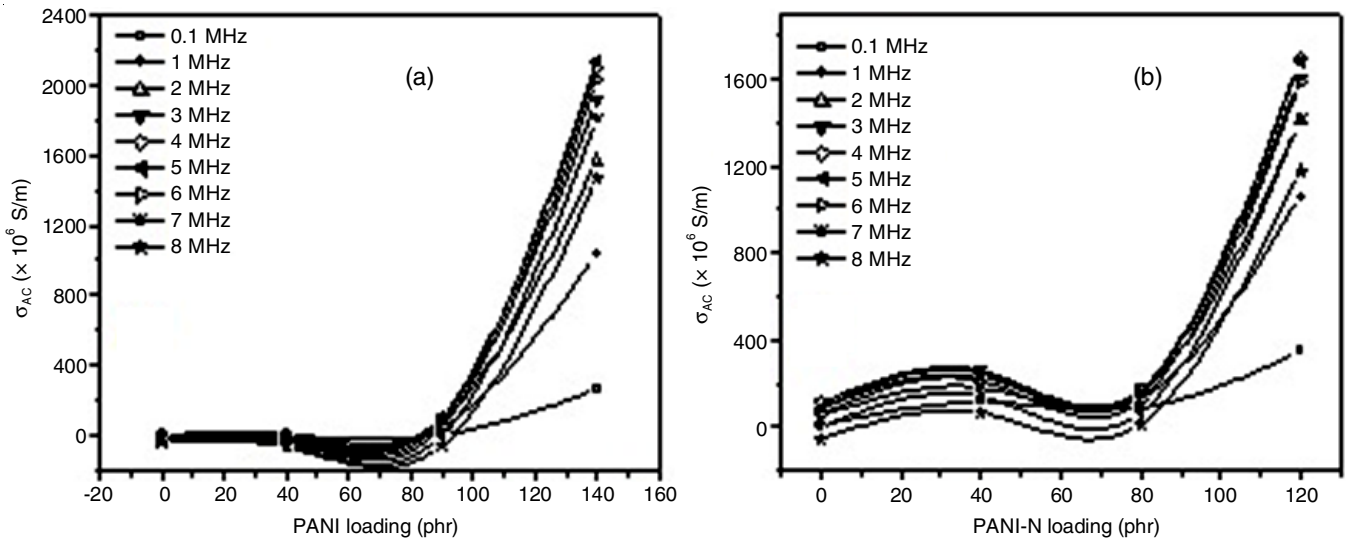

Fig. 16. Effect of loading on AC conductivity of CPCs (a) PANI, (b) PANI-N

primary cause of the conductivity in CPCs is charge carrier hopping. AC conductivity increases with increase in frequency and temperature and drops after reaching a maximum for the CPCs due to an increase in hopping conduction. A maximum conductivity of 2.13×10^{-3} S/m at 5 MHz is observed for the CPCs at 140 phr PANI loading. The 120 phr PANI-N-loaded CPC gives conductivity (1.68×10^{-3} S/m) very close to the 140 phr PANI-loaded CPC at the same frequency. Thus, the dielectric properties of the rubber matrix can be modified by appropriate loadings of PANI and PANI-N according to the intended operating temperature and frequency.

CONFLICT OF INTEREST

The author declare that there is no conflict of interests regarding the publication of this article.

REFERENCES

1. A. Bhattacharya and A. De, *Prog. Solid State Chem.*, **24**, 141 (1996); https://doi.org/10.1016/0079-6786(96)00002-7
2. S.F. Al-Sarawi, D. Abbott and P.D. Franzon, *IEEE Trans. Compon. Packag. Manuf. Technol. Part B Adv. Packag.*, **21**, 2 (1998); https://doi.org/10.1109/96.659500
3. J. Lu and C.P. Wong, *IEEE Trans. Dielectr. Electr. Insul.*, **15**, 1322 (2008); https://doi.org/10.1109/TDEI.2008.4656240
4. L. Variar, M.N. Muralidharan, S.K. Narayanankutty and S. Ansari, *J. Mater. Sci. Mater. Electron.*, **32**, 5908 (2021); https://doi.org/10.1007/s10854-021-05311-z
5. T. Dayyoub, A.V. Maksimkin, O.V. Filippova, V.V. Tcherdyntsev and D.V. Telyshev, *Polymers*, **14**, 3511 (2022); https://doi.org/10.3390/polym14173511
6. D. Dimos, S.J. Lockwood, R.W. Schwartz and M.S. Rodgers, *IEEE Trans. Compon. Packag. Manuf. Technol. Part A*, **18**, 174 (1995); https://doi.org/10.1109/95.370752
7. S.S. Pradhan, L. Unnikrishnan, S. Mohanty and S.K. Nayak, *J. Electron. Mater.*, **49**, 1749 (2020); https://doi.org/10.1007/s11664-019-07908-x
8. H. Xu, L. Huang, W. Li, S. Gu, D. Zeng, Y. Zhang, Y. Sun and H. Cheng, *J. Membr. Sci.*, **651**, 120452 (2022); https://doi.org/10.1016/j.memsci.2022.120452
9. T. Taka, *Synth. Met.*, **41**, 1177 (1991); https://doi.org/10.1016/0379-6779(91)91582-U
10. P. Tan, H. Wang, F. Xiao, X. Lu, W. Shang, X. Deng, H. Song, Z. Xu, J. Cao, T. Gan, B. Wang and X. Zhou, *Nat. Commun.*, **13**, 358 (2022); https://doi.org/10.1038/s41467-022-28027-y
11. J. Joo, S.M. Long, J.P. Pouget, E.J. Oh, A.G. MacDiarmid and A.J. Epstein, *Phys. Rev. B Condens. Matter*, **57**, 9567 (1998); https://doi.org/10.1103/PhysRevB.57.9567
12. M. Das, A. Akbar and D. Sarkar, *Synth. Met.*, **249**, 69 (2019); https://doi.org/10.1016/j.synthmet.2019.02.004
13. K. Dash, N.K. Hota and B.P. Sahoo, *J. Mater. Sci.*, **55**, 12568 (2020); https://doi.org/10.1007/s10853-020-04834-w
14. N.N. Rozik and S.L.A. El-Messieh, *Polym. Bull.*, **74**, 3595 (2017); https://doi.org/10.1007/s00289-017-1904-7
15. M.G. Han and S.S. Im, *J. Appl. Polym. Sci.*, **71**, 13 (1999); https://doi.org/10.1002/(SICI)1097-4628(19990328)71:13<2169:AID-APP7>3.0.CO;2-P
16. P.S. Mangali, D. Marcia, G. Marianna and B.G. Soares, *J. Appl. Polym. Sci.*, **71**, 14 (1999); https://doi.org/10.1002/(SICI)1097-4628(19990404)71:14<2329:AID-APP6>3.0.CO;2-Y
17. K. Pielichowski, *J. Therm. Anal. Calorim.*, **54**, 171 (1998); https://doi.org/10.1023/A:1010129205138
18. B.K. Sharma, N. Khare, S.K. Dhawan and H.C. Gupta, *J. Alloys Compd.*, **477**, 370 (2009); https://doi.org/10.1016/j.jallcom.2008.10.004
19. G. Joshi and S.M. Pawde, *J. Appl. Polym. Sci.*, **102**, 1014 (2006); https://doi.org/10.1002/app.24062
20. C. Min, X. Shen, Z. Shi, L. Chen and Z. Xu, *Polym. Plast. Technol. Eng.*, **49**, 1172 (2010); https://doi.org/10.1080/03602559.2010.496405
21. I. Plesa, P.V. Notingher, S. Schlögl, C. Sumereder and M. Muhr, *Polymers*, **8**, 173 (2016); https://doi.org/10.3390/polym8050173
22. S. Bhadra, N.K. Singha and D. Khastgir, *Curr. Appl. Phys.*, **9**, 396 (2009); https://doi.org/10.1016/j.cap.2008.03.009
23. Z. Elimat, *J. Compos. Mater.*, **49**, 3 (2015); https://doi.org/10.1177/0021998313514256
24. K. Ahmad, W. Pan and S.-L. Shi, *Appl. Phys. Lett.*, **89**, 133122 (2006); https://doi.org/10.1063/1.2357920
25. W. Zheng and S.-C. Wong, *Compos. Sci. Technol.*, **63**, 225 (2003); https://doi.org/10.1016/S0266-3538(02)00201-4
26. A.S. Chandran and S.K. Narayanankutty, *J. Mater. Res.*, **24**, 2728 (2009); https://doi.org/10.1557/jmr.2009.0329
27. A.S. Chandran and S.K. Narayanankutty, *Polym. Plast. Technol. Eng.*, **50**, 443 (2011); https://doi.org/10.1080/03602559.2010.543225
28. A. Goswamy, Thin Film Fundamentals, New Age International Publishers Ltd., New Delhi (1996).
29. C. Ramasasstry and Y.S. Rao, *J. Phys. E Sci. Instrum.*, **12**, 1023 (1979); https://doi.org/10.1088/0022-3735/12/11/002
30. H.T. Lee, C.S. Liao and S.A. Chen, *Makromol. Chem.*, **194**, 2443 (1993); https://doi.org/10.1002/macp.1993.021940903
31. B.G. Soares, M.E. Leyva, G.M.O. Barra and D. Khastgir, *Eur. Polym. J.*, **42**, 676 (2006); https://doi.org/10.1016/j.eurpolymj.2005.08.013
32. G. Juarez-Martinez, A. Chiolerio, P. Allia, M. Poggio, C.L. Degen, L. Zhang, B.J. Nelson, L. Dong, M. Iwamoto, M.J. Buehler, G. Bratzel, F.A. Mohamed, N. Doble, A. Govil, I. Bita, E. Gusev, J.-T. Huang, K.-Y. Lee, H.-J. Hsu, P.-S. Chao, C.-Y. Lin, J. Muthuswamy, M. Okandan, D.P. Butler, Z. Celik-Butler, B. Kim, W.-T. Park, A. Baig, D. Gamzina, J. Zhao, Y. Shin, R. Barchfeld, L.R. Barnett, C. Domier, N.C. Luhmann, Y. Rosen, P. Gurman, C. Snoeyink, S.T. Wereley, R. Ghosh, A. Kumar, P.P. Mukherjee, S. Kim, T. Thundat, A. Gopal, K. Hoshino, J.X. Zhang, T. Ono, M. Esashi, S. Tsuda, R.M. Pocratsky, M.P. Boer, S. Litster, C.W. Padgett, T.S. Whiteside, L. Preziosi, S. Tsuda, M.A. Pasquinelli, Y.G. Yingling, Y. Shi, S.A. Boden, D.M. Bagnall, R.E. Serda and M. Ferrari, Maxwell–Wagner Effect, Encyclopedia of Nanotechnology, Dordrecht: Springer Netherlands, pp. 1276–1285 (2012); https://doi.org/10.1007/978-90-481-9751-4_5
33. C.G. Koops, *Phys. Rev.*, **83**, 121 (1951); https://doi.org/10.1103/PhysRev.83.121
34. J. Maxwell, Electricity and Magnetism, Oxford University Press: London, vol. 1, Section 328 (1873).
35. K. Wagner, *Ann. Phys.*, **345**, 817 (1913); https://doi.org/10.1002/andp.19133450502
36. B. Tareev, Physics of Dielectrics, Mir Publishers, Moscow (1979).
37. C.P. Smyth, Dielectric Behavior and Structure, McGraw-Hill Book Company Inc.: New York, p. 191 (1955).
38. N.G. McCrum, B.E. Read and G. Williams, Anelastic and Dielectric Effects in Polymeric Solids, John Wiley & Sons: New York, p. 211 (1967).
39. E. Riande and R.D. Calleja, Electrical Properties of Polymers, Hanser Publishers: Munich, Germany, p. 34 (1987).
40. C.C. Ku and D. Liepins, Electrical Properties of Polymers, Carl Hanser Verlag: Munich (1987).
41. E.S. Matveeva, I. Hernández-Fuentes, V. Parkhutik and R. Díaz-Calleja, *Synth. Met.*, **79**, 181 (1996); https://doi.org/10.1016/S0379-6779(97)80075-6
42. R. Diaz Calleja, E.S. Matveeva and V.P. Parkhutik, *J. Non-Cryst. Solids*, **180**, 260 (1995); https://doi.org/10.1016/0022-3093(94)00470-6
43. H.T. Lee, K.R. Chuang, S.A. Chen, P.K. Wei, J.H. Hsu and W. Fann, *Macromolecules*, **28**, 7645 (1995); https://doi.org/10.1021/ma00127a009
44. M.G. Han and S.S. Im, *J. Appl. Polym. Sci.*, **82**, 2760 (2001); https://doi.org/10.1002/app.2129

45. P. B. Macedo, C. T. Moynihan and R. Bose, *Phys. Chem. Glasses*, **13**, 171 (1972).
46. M.K. Ram, S. Annapoorni, S.S. Pandey and B.D. Malhotra, *Polymer*, **39**, 3399 (1998); https://doi.org/10.1016/S0032-3861(97)10285-3
47. K.A. Malini, Ph.D. Thesis, Studies on the Structural, Electrical and Magnetic Properties of Composites Based on Spinel Ferrites, Department of Physics, Cochin University of Science and Technology, Cochin, India (2001).
48. A.M. Jeffery and D.H. Damon, *IEEE Trans. Dielectr. Electr. Insul.*, **2**, 394 (1995); https://doi.org/10.1109/94.395428
49. K.S. Cole and R.H. Cole, *J. Chem. Phys.*, **9**, 341 (1941); https://doi.org/10.1063/1.1750906
50. A.M.Y. El-Lawindy, *Egypt. J. Solids*, **28**, 97 (2005); https://doi.org/10.21608/EJS.2005.149350
51. F.E. Karasz, Dielectric properties of Polymers, Plenum Press: New York (1972).
52. K.C. Han, H.D. Choi, T.J. Moon, W.S. Kim and K.Y. Kim, *J. Mater. Sci.*, **30**, 3567 (1995); https://doi.org/10.1007/BF00351866
53. K. Lichtenecker, *Phys. Z.*, **10**, 1005 (1908).
54. L. Liang, X. Feng, J. Liu and P.C. Rieke, *J. Appl. Polym. Sci.*, **72**, 1 (1999); https://doi.org/10.1002/(SICI)1097-4628(19990404)72:1<1::AID-APP1>3.0.CO;2-B
55. M.E. Achour, M.E.L. Malhi, J.L. Miane, F. Carmona and F. Lahjomri, *J. Appl. Polym. Sci.*, **73**, 969 (1999); https://doi.org/10.1002/(SICI)1097-4628(19990808)73:6<969::AID-APP14>3.0.CO;2-1
56. K.W. Wagner, *Arch. Elektrotech.*, **3**, 67 (1914); https://doi.org/10.1007/BF01657563
57. M. George, Ph.D. Thesis, Investigations on the Finite Size Effects of Some Inverse Spinels and Studies on their Composites Based on Nitrile Rubber, Department of Physics, Cochin University of Science & Technology, Cochin, India (2004).
58. M.A. Ahmed, M.A. El Hiti, M.K. El Nimr and M.A. Amer, *J. Magn. Magn. Mater.*, **152**, 391 (1996); https://doi.org/10.1016/0304-8853(95)00479-3
59. A.K. Jonscher, *Thin Solid Films*, **36**, 1 (1976); https://doi.org/10.1016/0040-6090(76)90388-6
60. J. Tauc, Optical Properties of Solids, Springer: Boston, USA, pp. 123-136 (1969).
61. M.A. Hiti, *J. Phys. D Appl. Phys.*, **29**, 501 (1996); https://doi.org/10.1088/0022-3727/29/3/002
62. R. Singh, R.P. Tandon, G.S. Singh and S. Chandra, *Philos. Mag. B Phys. Condens. Matter Stat. Mech. Electron. Opt. Magn. Prop.*, **66**, 285 (1992); https://doi.org/10.1080/13642819208224590
63. R. Singh, A.K. Narula, R.P. Tandon, A. Mansingh and S. Chandra, *J. Appl. Phys.*, **79**, 1476 (1996); https://doi.org/10.1063/1.360987
64. E. Punkka, M.F. Rubner, J.D. Hettinger, J.S. Brooks and S.T. Hannahs, *Phys. Rev. B Condens. Matter*, **43**, 9076 (1991); https://doi.org/10.1103/PhysRevB.43.9076
65. M. Reghu, Y. Cao, D. Moses and A.J. Heeger, *Phys. Rev. B Condens. Matter*, **47**, 1758 (1993); https://doi.org/10.1103/PhysRevB.47.1758
66. B. Sixou, N. Mermilliod and J.P. Travers, *Phys. Rev. B Condens. Matter*, **53**, 4509 (1996); https://doi.org/10.1103/PhysRevB.53.4509
67. B. Sixou, J.P. Travers and Y.F. Nicolau, *Synth. Met.*, **84**, 703 (1997); https://doi.org/10.1016/S0379-6779(96)04113-6
68. D.V. Konarev, Y.V. Zubavichus, Y.L. Slovokhotov, Y.M. Shul'ga, V.N. Semkin, N.V. Drichko and R.N. Lyubovskaya, *Synth. Met.*, **92**, 1 (1998); https://doi.org/10.1016/S0379-6779(98)80000-3